Morphology and Physical Properties of Poly(butylene Terephthalate)

ENG-PI CHANG and EUGENE L. SLAGOWSKI, *Hooker Research Center, Hooker Chemicals & Plastics Corporation, Niagara Falls, New York 14302*

Synopsis

Liquid nitrogen-quenched PBT samples produce much larger spherulites of an optic axis orientation different from that of the air-cooled samples. Optical and scanning electron microscopy show that glass fibers in the glass-reinforced PBT sample nucleate the growth of well-defined spherulites along the glass fiber axis. Fracture studies at temperatures below and above the T_g indicate, respectively, brittle and ductile interspherulite boundary fracture. From dynamic mechanical studies, three transitions designated by α (flow transition), β (T_g), and γ (secondary relaxation) are observed. The magnitudes of the β and γ transitions are larger for the more amorphous quenched sample than the air-cooled sample, suggesting their amorphous phase origin. Addition of glass fibers raises the dynamic modulus and flow temperature, but suppresses the γ transition without significantly affecting the melting and glass transition temperatures.

INTRODUCTION

The growing importance of poly(butylene terephthalate) (PBT) as an engineering thermoplastic has resulted in an increasing number of recent publications on this polymer. Gilbert and Hybart[1] have studied the isothermal crystallization kinetics and mechanisms, while Stein et al.[2,3] have elucidated its superstructures crystallized at different temperatures by optical methods. Macrodeformation of superstructures during cold rolling has been observed by Wilkes and Chu,[5] while crystal lattice deformation during stretching has been inferred from x-ray diffraction.[6] In addition, the effect of skin-core morphology has also been correlated with the fracture nature by Hobbs and Pratt,[4], and processing variables have been demonstrated to affect the rheological properties and impact strength.[7] The effects of molecular weight, glass fiber length, and orientation on mechanical properties have also been studied by McNally and Freed.[8] The purpose of this paper is to investigate the effect of liquid nitrogen quenching and glass reinforcement on the morphology, degree of crystallinity, and dynamic mechanical properties of PBT.

EXPERIMENTAL

Materials

The PBT used in this study was a Goodyear material with the trade name of VFR 4716, which has a $\overline{M}_w = 45{,}000$, $\overline{M}_w/\overline{M}_n \approx 2$, and $[\eta] = 0.8$ (in 60% phenol, 40% tetrachloroethane).

The glass-reinforced PBT (GR-PBT) sample contains 30 wt-% glass fiber (Johns Manville, type E, JM 303.13, $^3/_{16}$ in. chopped strands) treated with a

Journal of Applied Polymer Science, Vol. 22, 769–779 (1978)

0021-8995/78/0022-0769$01.00

proprietary sizing agent and extruded and pelletized in a Werner and Pfleiderer twin-screw extruder. The subsequent composite was screw injection molded at ~250°C in an Arburg 200 molding maching in the form of tensile bars which were used for film preparation.

Film Preparation

Films were pressed on a Carver press at 260°C for 3 min under 10,000 lb force, giving a film thickness of about 0.15 mm. The PBT and the glass-filled PBT samples were removed and cooled to room temperature (air-cooled samples). One premelted PBT sample was quenched in liquid N_2 (quenched sample).

Solution-cast films were obtained by casting a 10% CF_3COOH solution on glass slides followed by relatively fast evaporation in a covered Petri dish.

Dynamic Mechanical Measurements

Dynamic mechanical measurements were made at 110 hertz with the Rheo-Vibron (TOYO Company, Model DDV-II) over a temperature range of −120°–230°C. The heating rate was about 1°C/min.

Density Measurement

The density of the film samples was determined by a density gradient column of aqueous potassium iodide solution of densities ranging from 1.25 to 1.40. Weight fraction of crystallinity is calculated from the relation

$$\beta = d_c(d - d_{am})/d(d_c - d_{am})$$

where d, d_c, and d_{am} are the sample, crystal, and amorphous densities, respectively.

Optical and Scanning Electron Microscopy

Optical micrographs were obtained on thin film samples with a Reichert Zetopan microscope under crossed polaroid conditions. Scanning electron microscopy studies were carried out with a JEOL JSM 50A scanning electron microscope.

Differential Scanning Calorimetry

Thermal analyses were pursued on a Perkin-Elmer DSC-2 calorimeter. About 15 to 20-mg samples were placed in an aluminum pan with a lid. The heating rate was 10°C/min under an N_2 flow of 40 cc/min.

Wide-Angle X-Ray Diffraction (WAXD)

WAXD was carried out with a Phillips Norelco diffractometer in the reflectance mode. This is equipped with an Advanced Metal Research focusing monochromater fitted with a graphite crystal and a proportional detector. Bragg angle 2θ scans from 4° to 40° were obtained at a speed of 1°/min. The scattering pattern was recorded directly on a strip chart with a speed of ½ in./min.

Small-Angle Laser Scattering (SALS)

The SALS apparatus[9] consisted of a Spectra Physics continuous wave He–Ne laser (Model 133P, λ = 6328 Å), a polarizer, and an analyzer. The scattering envelope was recorded on Polaroid Type 55 (4 in. × 5 in.) films. H_v patterns were taken with the polarizer vertical and the analyzer horizontal.

RESULTS AND DISCUSSION

Morphology

Figures 1(a) to 1(c) show the optical micrographs of the air-cooled, quenched, and air-cooled GR-PBT samples, respectively, while Figure 1(d) shows the corresponding SALS-H_v pattern of the quenched sample. For the air-cooled PBT and GR-PBT samples, microspherulites of 1–2 μ and 5–6 μ diameters were observed in the optical micrographs, although no well-defined H_v pattern was observed for these two samples. In recent work of Misra and Stein,[2] H_v pattern arising from spherulites formed at 0°–180°C showed 0°–90° oriented four lobes, while those crystallized at higher temperatures showed the 45° oriented pattern. It is interesting to note that in the present quenched sample, a distinct 0°–90° H_v pattern indicative of spherulites with optic axes inclined at 45° to the spherulite radii was obtained. Such a 0°–90° oriented pattern can be rationalized by the poor heat transfer of the liquid nitrogen medium which results in inefficient quenching (~8%–9% crystallinity as determined by density and x-ray

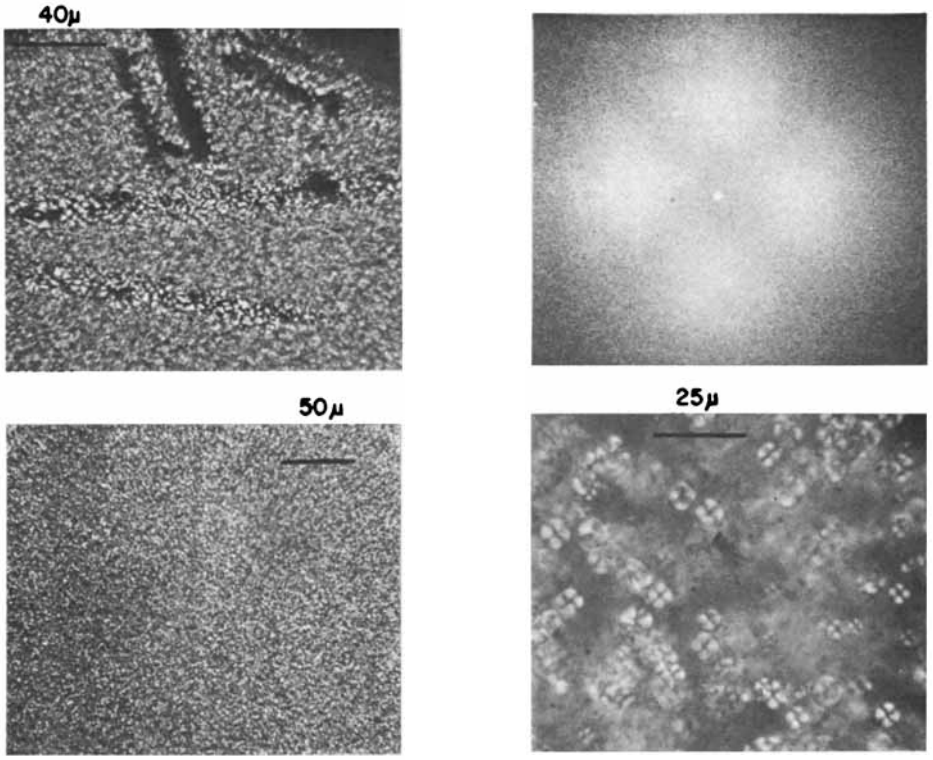

Fig. 1. Cross-polaroid optical micrographs of (a) air-cooled, (b) liquid N_2-quenched, and (c) air-cooled glass reinforced PBT sample. (d) H_v Pattern of liquid N_2-quenched sample.

diffraction). It is also noteworthy that this quenched sample shows comparatively larger spherulites (5–6 μ) than the air-cooled sample together with a distinct Maltese cross in the optical micrograph Figure 1(b). It is conceivable that such quenched samples would be of a similar nature as those crystallized by Misra and Stein at the low temperatures.[2]

Figures 2(a) to 2(d) show the corresponding optical micrographs and H_v patterns of the (~10% in CF_3COOH) control and GR samples. It is evident that very well-defined spherulites (20–40 μ) are observed. It is also interesting to note [Fig. 2(b)] that most of the PBT spherulites grow along the glass fibers suggestive of the nucleating ability of the glass fiber. The distinct four-leaf clover H_v patterns with maxima at azimuthal angle of 45° confirms the spherulitic morphology and are in agreement with those reported previously.[2]

Etching and Fracture Studies

Figure 3(a) shows the SEM picture of the solution-cast PBT sample. This sample, after etching with chromic acid for 10 min, shows attacked areas of radial and peripheral cracks [Fig. 3(b)]. If it can be assumed that the etching selectively

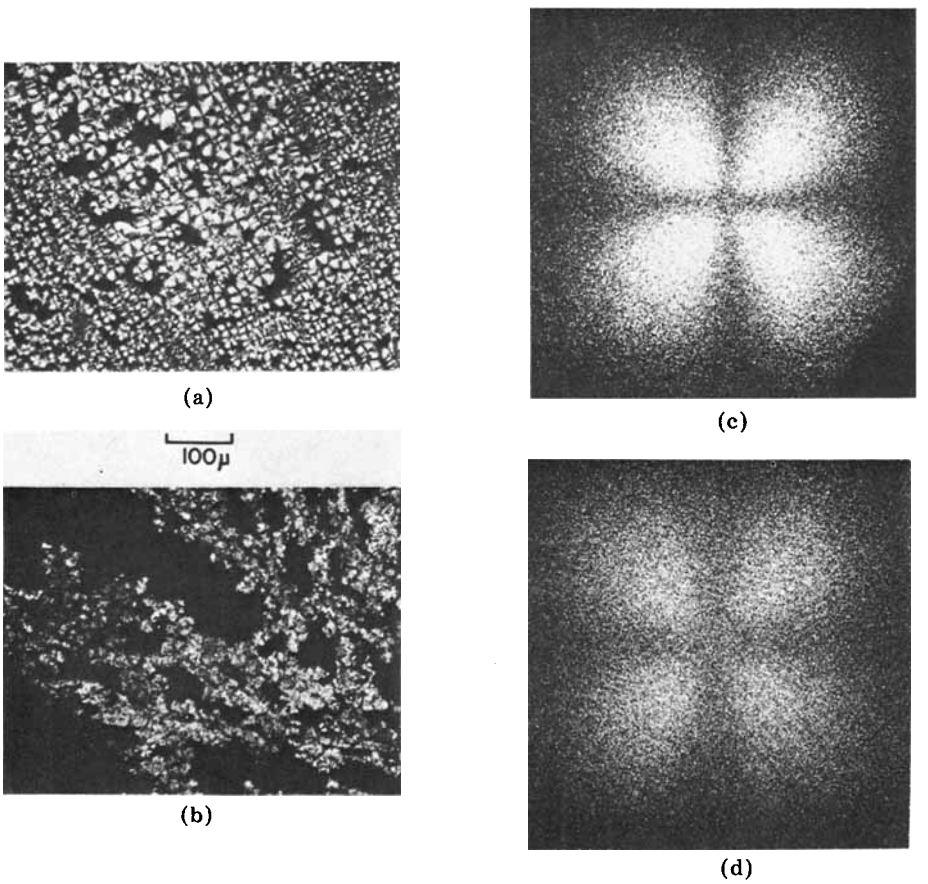

Fig. 2. Cross-polaroid optical micrographs and H_v patterns of solution-cast PBT films: (a) and (c), PBT; (b) and (d), GR-PBT.

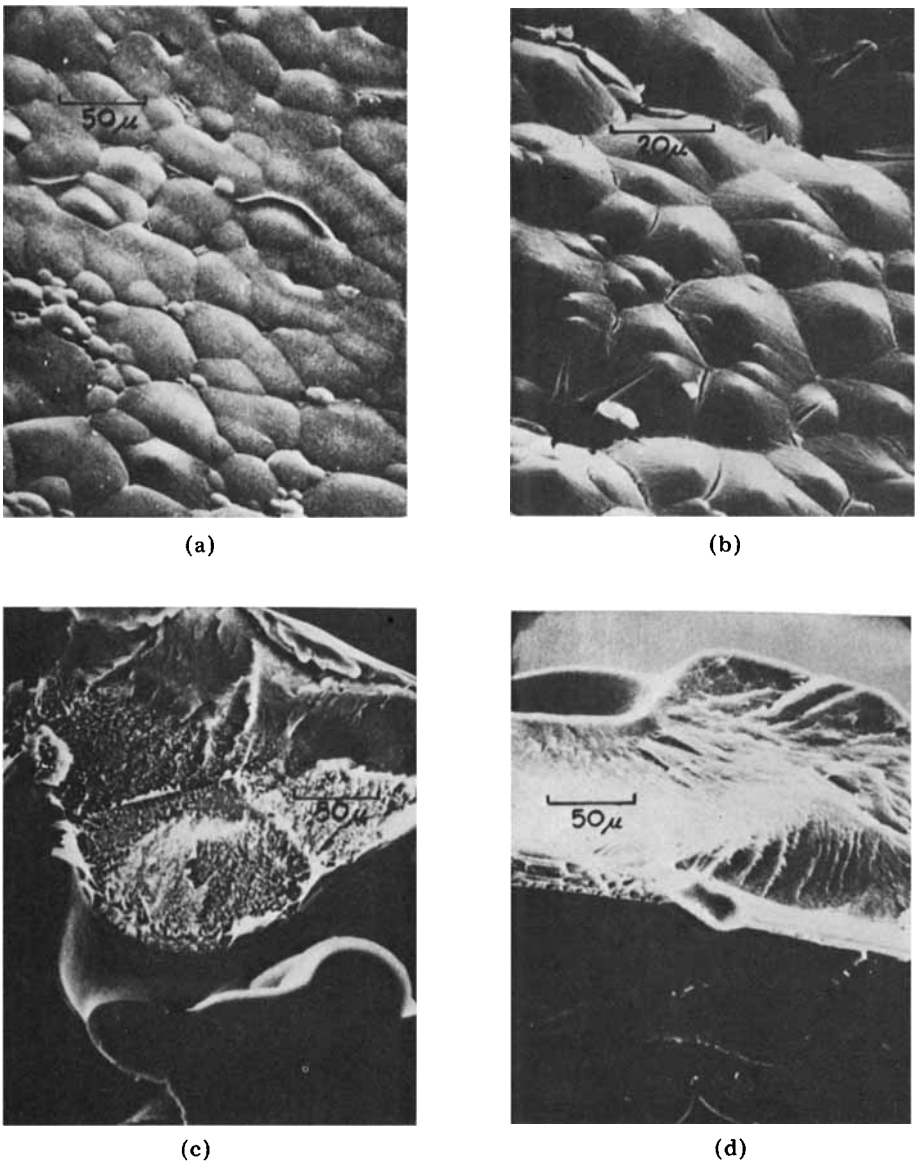

Fig. 3. SEM pictures of solution-cast PBT film (a) before etching, (b) after 10 min of etching with chromic acid, (c) fractured at 90°C, and (d) fractured at liquid N_2 temperature.

attacks the amorphous region, this would suggest the preferential localization of the amorphous phase in the radial direction of interspherulite boundaries.

The morphology of this solution-cast PBT sample fractured above (at 90°C) and below its T_g (at liquid N_2 temperature) is shown in Figures 3(c) and 3(d), respectively. When fractured below its T_g, the morphology suggests a brittle fracture along the spherulite boundaries, while boundary fracture of a more ductile nature is observed when the sample is fractured at 90°C.

Figure 4(a) shows the corresponding SEM picture of the solution-cast GR sample. In confirmation with the previously described optical microscopy results, the nucleating nature of the glass fiber is apparent from the growth of the

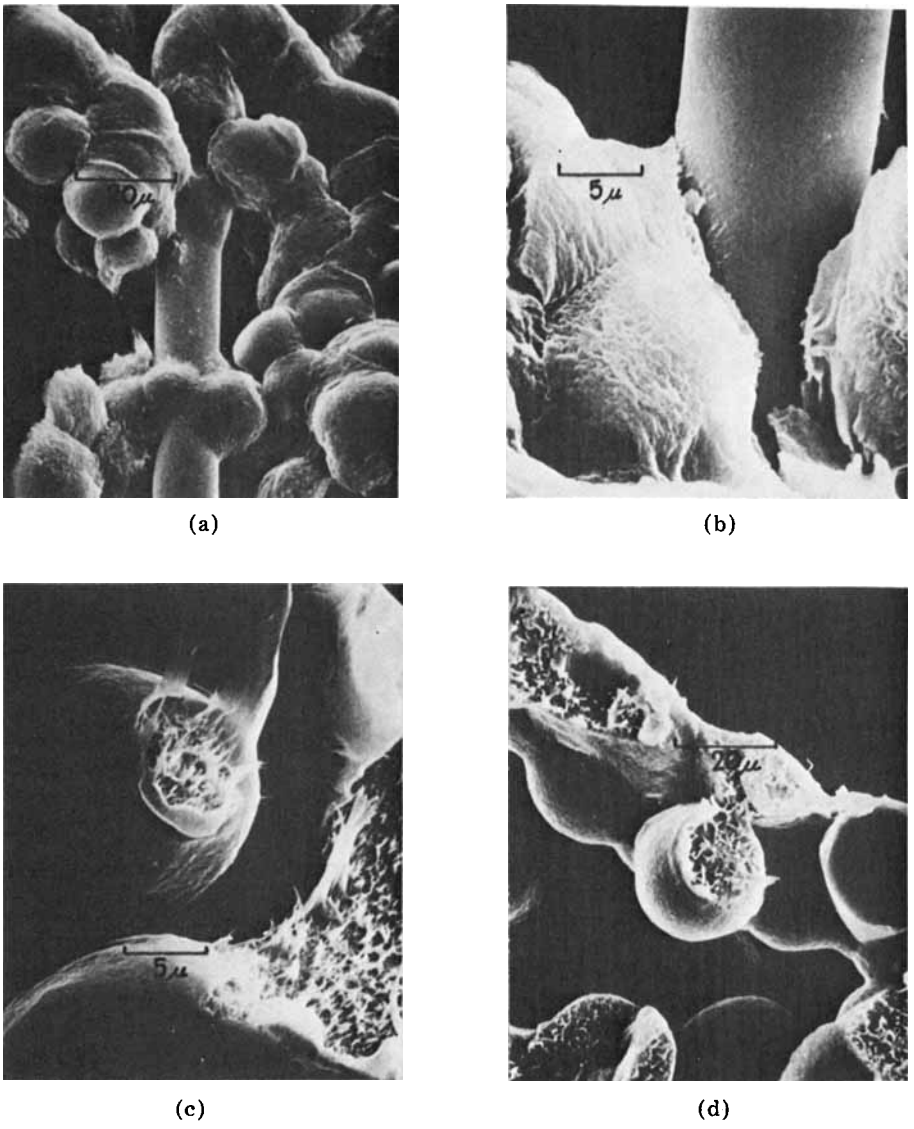

Fig. 4. SEM pictures of solution-cast GR-PBT film (a) before etching, (b) after 10 min of etching with chromic acid, (c) fractured at 90°C, and (d) fractured at liquid N_2 temperature.

PBT spherulites along the glass fiber. The 10-min chromic acid-etched sample shows distinct dislocation at the joints of the spherulites and the glass fibers, suggesting preferential attack of the bonding region [Fig. 4(b)]. Figures 4(c) and 4(d) show similar fracture studies above and below the T_g of this GR sample. Boundary fracture with ductile and brittle nature is again observed.

Crystallinity

Figures 5(a) to 5(c) show the Bragg angle scans of the air-cooled quenched and air-cooled GR-PBT samples. Strong diffraction peaks are observed at $2\theta = 16.0°$, 17.3°, 20.6°, 23.4°, and 25.2°. Some weak diffraction peaks are also apparent

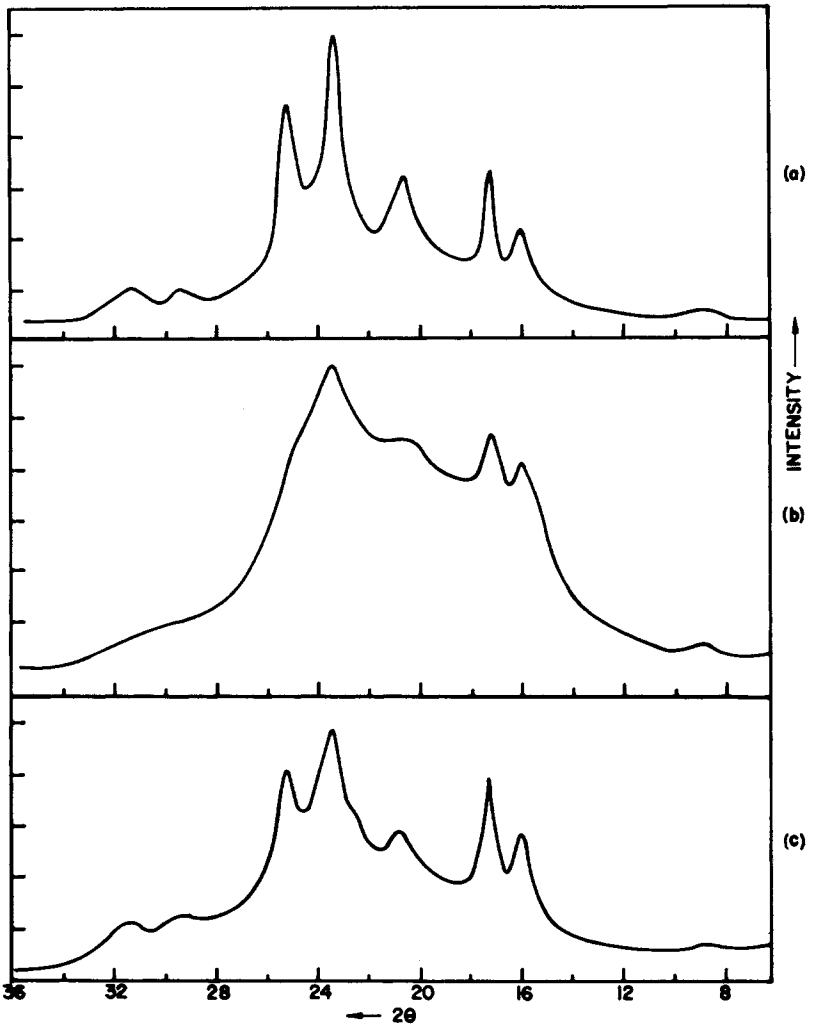

Fig. 5. X-Ray diffraction patterns of PBT films (a) air-cooled, (b) liquid N_2-quenched, and (c) air-cooled glass-reinforced.

at $2\theta = 9°$, 29.4°, and 31.3° for the air-cooled PBT and GR-PBT samples. The diffraction pattern is in good agreement with the triclinic unit cell structure reported by Joly et al.,[10] Jakeway et al.,[6] and Hobbs et al.[4] These patterns are then separated into areas attributed to background, amorphous, and crystalline scattering by the following procedure. An air-scattering scan was obtained for background correction. For the amorphous area contribution, ice water-quenched samples of PBT ($\rho = 1.280$) and GR-PBT which show only amorphous scattering were used for the amorphous correction for the corresponding samples. The intensity was normalized for thickness and amorphous content as determined from the density method. Weight fraction of crystallinity is determined from the equation

$$X_C = \frac{\Sigma I_C}{\Sigma I_C + I_A}$$

where ΣI_C = sum of integrated intensities of crystalline peaks and I_A = integrated intensity of the amorphous peak. The resuts are compared with those obtained by density method ($\rho_{amorphous} = 1.280$; $\rho_{crystalline} = 1.396$)[2] in Table I. It is apparent that the agreement between the two methods is excellent. The surprisingly substantial percentage of crystallinity of the quenched sample is, as previously mentioned, due to the poor heat transfer of liquid nitrogen, which results in inefficient quenching. The presence of glass fiber does not significantly affect the overall percentage of crystallinity of PBT.

Dynamic Mechanical Properties

Figure 6 compares the temperature dependence of the dynamic storage modulus E' for the three samples. The glass-reinforced sample shows the highest E throughout the temperature range due to the reinforcing nature of the glass fibers. At −120°C, its E' value is about 30% higher than that of the quenched or air-cooled sample. However, as the temperature increases, the reinforcing effect due to the glass fibers becomes more pronounced. At 130°C, the glass-reinforced sample has an E' five times that of the quenched sample and three times that of the air-cooled sample. Near the T_g of PBT (~60°C), the E' of the quenched sample drops more sharply than the more crystalline air-cooled sample. The crystallites in the air-cooled sample act as a modulus-reinforcing filler.

Figure 7 shows the corresponding temperature dependence of the dynamic loss modulus (E'') for the three samples. Three transitions are apparent: (1) the flow or α transition at ~205°–215°C, which can be associated with the onset of the melting of the crystallites; (2) the β transition at ~60°C, which is the T_g, and (3) a secondary relaxation, γ transition, at ~−80°C. The quenched sample shows a very indistinct shoulder at ~205°C. In comparing the two pure PBT samples, the magnitude of the β and γ transitions decreases with increased degree of crystallinity. With the addition of glass fibers, the loss modulus (E'') value relative to the pure PBT was raised because of the pronounced increase in E'. The presence of the glass fibers delays the flow or deformation of the crystallites, leading to a higher α-transition temperature. The suppression of the γ transition in the GR sample is evident by the indistinct shoulders present in the −40° to −100°C region. This transition has been attributed to the superposition of several processes[11] involving most probably the

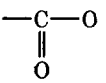

and or the glycol residue. It is possible that the adhesion of the glass fibers with PBT greatly restricts these local relaxations at the boundary interfaces, and the multiple shoulders observed in the γ-transition region could be attributed to the heterogeneous environment of the PBT chains which gives rise to a spectrum distribution of relaxation times.

Table I summarizes the transition temperatures of the three samples determined from Vibron and DSC. It can be seen that the presence of glass fiber does not significantly affect the T_g and the melting point but raises the flow transition temperature indicative of a reinforcing filler character.

TABLE I
Transition Temperatures and Percentage of Crystallinity of PBT Samples

PBT sample	Transition temperature, °C					% Crystallinity	
	γ From E''_{max}	β From E''_{max}	β DSC	α From E''_{max}	Melting DSC	X-ray diffraction	Density
Air cooled	−85 (broad)	60	44	206	224.5	32.0	31.0
Liquid N_2 quenched	−85 (broad)	60	44	206 (shoulder)	224.5[a]	8.0	9.5
30% Glass reinforced	indistinct	60	45	216	224	30.0	—

[a] Recrystallized during scan.

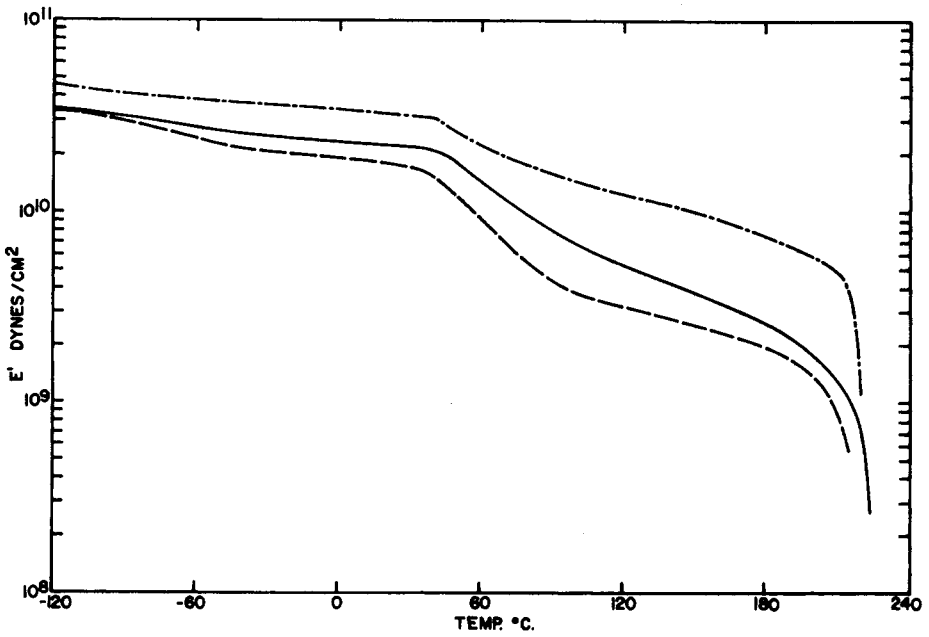

Fig. 6. Temperature dependence of dynamic storage modulus E' of PBT films: (—) air-cooled; (— —) liquid N_2-quenched; (— .) air-cooled glass-reinforced.

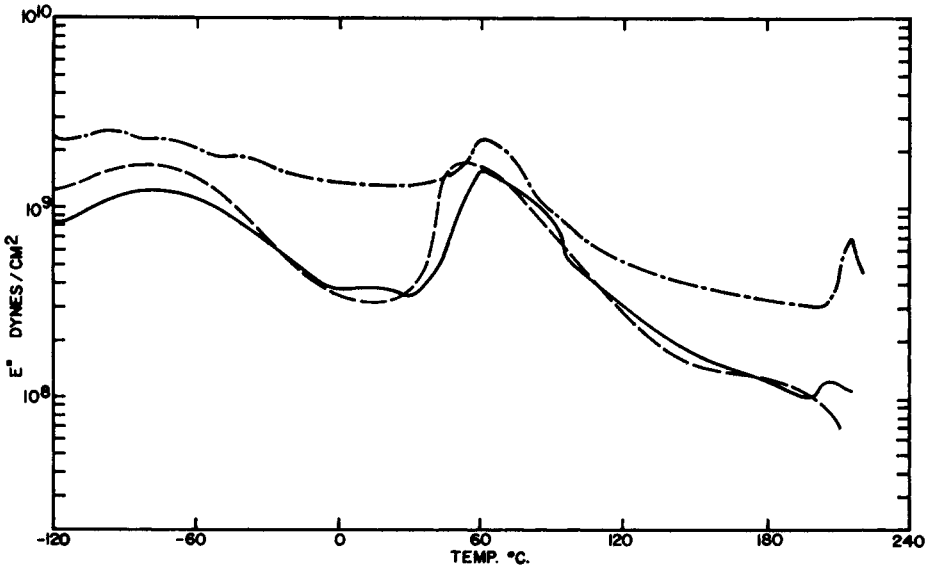

Fig. 7. Temperature dependence of dynamic loss modulus E'' of PBT films: (—) air-cooled; (— —) liquid N_2-quenched; (— .) air-cooled glass-reinforced.

CONCLUSIONS

A well-defined spherulitic morphology was observed with solution-cast PBT and PBT samples reinforced with glass fibers which act as nucleating sites. Fracture studies of these samples at temperatures below and above the T_g indicate brittle and ductile interspherulite boundary fracture, respectively.

In the dynamic mechanical studies, three transitions, α (flow transition), β

(T_g), and γ (secondary relaxation), were observed in the air-cooled, quenched, and glass-reinforced PBT samples. The magnitude of the β and γ transitions are larger for the more amorphous quenched sample. The addition of glass fiber raises the dynamic modulus; the flow temperature suppresses the γ transition but does not significantly affect the T_g and melting temperature of PBT.

The authors would like to thank Rudy Kirsten, Lynn Williams, Remy Cortellucci, and Irene Zsolnay for technical assistance and Anthony Lemper, Joseph Pawlak, and Jim Tkacik of the Hooker Research Center and Professor William MacKnight of the University of Massachusetts for valuable discussions.

References

1. M. Gilbert and F. J. Hybart, *Polymer,* **13,** 327 (1972).
2. A. Misra and R. S. Stein, *Bull. Am. Phys. Soc., Ser. II,* **20,** 341 (1975).
3. A. Wasiak and R. S. Stein, *Polym. Prepr.,* **16**(No. 2), 643 (1975).
4. S. Y. Hobbs and C. F. Pratt, *J. Appl. Polym. Sci.,* **19,** 1701 (1975).
5. G. L. Wilkes and C. M. Chu, *J. Appl. Polym. Sci.,* **18,** 2221 (1974).
6. R. Jakeways, I. M. Ward, M. A. Wilding, I. H. Hall, I. J. Desborough, and M. G. Pass, *J. Polym. Sci., Polym. Phys.,* **13,** 799 (1975).
7. M. P. Van Der Wielen, *Polym. Eng. Sci.,* **15**(No. 2), 17 (1975).
8. Donald McNally and W. T. Freed, *SPE Tech. Papers,* **20,** 79 (1974).
9. R. S. Stein in *Newer Methods of Polymer Characterization,* Bacon Ke, Ed., Interscience, New York, 1964, Chap. 4.
10. A. M. Joly, G. Nemoz, A. Douillard, and G. Vallet, *Makromol. Chem.,* **176,** 479 (1975).
11. K. H. Illers and H. Brener, *J. Colloid Sci.,* **18,** 1 (1963).

Received November 12, 1976
Revised December 15, 1976